Cancer Immunol Immunother (1999) 47:321–329

ORIGINAL ARTICLE

Michael C. Chan · Regina M. Murphy

Kinetics of cellular trafficking and cytotoxicity of 9.2.27-gelonin immunotoxins targeted against the high-molecular-weight melanoma-associated antigen

Received: 30 July 1998 / Accepted: 7 October 1998

Abstract The high-molecular-weight melanoma-associated antigen (HMW-MAA) is expressed on a large majority of melanoma tissues but not on most normal or other neoplastic tissues. Monoclonal antibody 9.2.27 binds with high affinity and specificity to the HMW-MAA, making it an attractive choice as an agent for targeting toxins or chemotherapeutic agents specifically towards melanomas. To characterize the interactions between 9.2.27 and melanoma cells more carefully, data on the kinetics of binding, internalization, and degradation of 9.2.27 by SK-MEL-2 cells were collected. Binding of 9.2.27 to SK-MEL-2 cells was rapid, and followed by slow loss of surface-bound antibody, probably because of loss of surface antigen caused by degradation and/or shedding. A small fraction (approx. 5%) of surface-bound 9.2.27 was internalized and degraded. A mathematical model describing these interactions was developed, and equilibrium and kinetic constants were fitted to the data. To evaluate the utility of 9.2.27 as a toxin-targeting agent, 9.2.27-gelonin immunotoxins were constructed and tested in protein synthesis inhibition assays. The dependence of the toxicity data for 9.2.27-gelonin on time and concentration was quantitatively related to the accumulated intracellular exposure to 9.2.27-gelonin by a relatively simple equation. This equation had been previously validated for immunotoxins targeted against the transferrin receptor, for which the trafficking kinetics are quite dissimilar from those of the HMW-MAA. The success of the approach here suggests that this method may be widely applicable for analysis of immunotoxin efficacy.

Key words Immunotoxins · Melanoma antigens · Cellular processing

M.C. Chan · R.M. Murphy (✉)
Department of Chemical Engineering,
1415 Engineering Drive, Madison, WI 53706, USA
e-mail: murphy@che.wisc.edu
Tel.: +1-608-262-1587 Fax: +1-608-262-5434

Introduction

The high-molecular-weight melanoma-associated antigen (HMW-MAA) is an integral membrane chondroitin sulfate proteoglycan that is expressed strongly and consistently on several melanoma cell lines and on virtually all melanoma tissue from patients, but is absent from healthy tissues and most non-melanoma cancers [2, 25, 26]. The monoclonal antibody 9.2.27 recognizes both the core 250-kDa glycoprotein and the 400-kDa proteoglycan forms of HMW-MAA [15]. The high affinity [28] and specificity [22] of 9.2.27 for the HMW-MAA make it a good candidate for use in immunotoxin therapy. Several 9.2.27-toxin conjugates have been generated and tested. A 9.2.27-gelonin immunotoxin [3] and a 9.2.27-vinblastine conjugate [27] inhibited tumor growth in vivo. In vitro, conjugates of 9.2.27 and the toxins ricin, abrin, and *Pseudomonas* exotoxin A demonstrated widely variable toxicity, with immunotoxin efficacy depending on the cell line, toxin, internalization rate, and intracellular processing of the toxin [10–13, 29].

Our laboratory has been developing methodologies for quantitatively relating the kinetics of toxicity of immunotoxins to the underlying rates of cellular processing. In previous work, a mathematical model was developed describing the protein synthesis inhibition activity of gelonin immunotoxins internalized by the transferrin receptor (TfR) [34, 35]. This experimentally validated model related protein synthesis inhibition of immunotoxins targeted against the TfR to the cellular trafficking kinetics of anti-TfR antibodies or transferrin. To determine the general applicability of this approach we have used it with the 9.2.27/HMW-MAA system. As targets for immunotoxin therapy, HMW-MAA and TfR display substantively different properties. HMW-MAA is believed to be an adhesion molecule involved in cell/cell and cell/substratum interactions [14, 16], and is not actively endocytosed. In contrast, TfR is rapidly internalized and then recycled to the cell surface in the iron-transport cycle [6]. HMW-MAA is constitutively shed

into the culture medium [7, 9, 23], whereas TfR is not shed. TfR is expressed at high density on many cancer cells but is also widely distributed on normal tissue [32], thus making it less than ideal as a specific tumor marker. HMW-MAA expression is almost exclusively restricted to melanoma and a few other kinds of tumor tissue [2, 22, 27]. This comparison should provide a fairly stringent test of the model structure.

In work described here, the cellular trafficking kinetics of mAb 9.2.27 were measured in SK-MEL-2 cells. A simple cellular trafficking model describing the kinetic processing of 9.2.27 by SK-MEL-2 cells was developed. A 9.2.27-gelonin immunotoxin was constructed and the kinetics of protein synthesis inhibition at various concentrations was measured. The kinetics of protein synthesis inhibition by the immunotoxin could be readily correlated to the kinetics of cellular processing of 9.2.27, using a previously derived expression [34]. The derived rate constant for translocation of 9.2.27-gelonin immunotoxins was of similar magnitude to that for anti(transferrin-receptor)–gelonin immunotoxins. The model describes the data for this system well, indicating that this methodology may be broadly applicable for the analysis and prediction of immunotoxin efficacy.

Materials and methods

Cells

SK-MEL-2 cells (American Type Culture Collection, Rockville, Md.) were maintained in a humidified incubator at 37 °C, 5% CO_2 with culture medium in 75-cm^2 T flasks. The medium was composed of minimal essential medium supplemented with 10% fetal bovine serum, 3.6 mM L-glutamine (Sigma, St. Louis, Mo.), 100 units/ml penicillin, and 100 μg/ml streptomycin (unless noted, from Gibco, Gaithersburg, Md.). Flow cytometry experiments indicated that at least 95% of SK-MEL-2 cells bound 9.2.27 (P.T. Yazdi and R.M. Murphy, unpublished data).

To determine cell growth kinetics, SK-MEL-2 cells were harvested with 5% dimethylsulfoxide (DMSO)/0.53 mM EDTA in PBS; the suspension was diluted into fresh medium (without DMSO/EDTA) at approximately 1.7×10^5 cells/ml. Trypsin was avoided in harvesting because it cleaves the HMW-MAA receptor [28]. Samples of 3 ml were plated into 60-mm culture dishes and incubated for 24 h to allow cells to attach to the dishes, then the medium was replaced with 3 ml fresh medium. In some cases, the medium contained 2 nM or 10 nM 9.2.27. No effect of the antibody was observed on cell growth. Cells were harvested and counted with a hemacytometer at several times after addition of fresh medium. The data were fit to Eq. 1 [1]:

$$c = \frac{c_0 \exp(k_g t)}{1 - c_0 \beta [1 - \exp(k_g t)]} \quad (1)$$

where c is the cell number per dish, c_0 is the initial cell number, k_g is a growth constant, and $1/\beta$ is the stationary cell number. Values of $k_g = 1.67 \times 10^{-3}$ min^{-1} and $\beta = 8 \times 10^{-7}$ dish $cells^{-1}$ were estimated by a nonlinear regression fit of Eq. 1 to several sets of cell growth data. c_0 ranged from 3×10^5 to 9×10^5 cells/dish in various experiments.

mAb purification

mAb 9.2.27 was purified by protein A affinity chromatography (Pharmacia, Piscataway, N.J.) from the supernatant of hybridoma cells generously donated by Michael Flickinger at the University of Minnesota. Purity was confirmed by sodium dodecyl sulfate/polyacrylamide gel electrophoresis (SDS-PAGE) and Zorbax GF-250 size-exclusion (Mac Mod, Chadds Ford, Pa.) HPLC. Following the manufacturer's instructions, Iodo-beads (Pierce, Rockford, Ill.) were used to radiolabel antibody with ^{125}I (DuPont-New England Nuclear, Boston, Mass.). An absorption coefficient of 1.4 ml mg^{-1} cm^{-1} at 280 nm was used to determine mAb concentration.

Binding affinity

SK-MEL-2 cells were harvested with DMSO/EDTA as described above and resuspended in medium at 1.7×10^5 cells/ml. A 3-ml sample (5×10^5 cells) was added to each 60-mm culture dish and incubated for 24 h to allow cells to attach. The supernatant was replaced with 3 ml medium containing various concentrations of ^{125}I-labeled 9.2.27 at 37 °C or 4 °C for 0.5–1 h. Preliminary experiments indicated that equilibrium was reached within 15–30 min at 4 °C. The concentration of mAb in the supernatant was determined in a gamma counter (model 5002, Packard, Meriden, Conn.). Total cell-associated, surface-bound, and internal mAb were determined essentially as described in more detail elsewhere [34]. Briefly, the monolayer was washed three times with cold PBS and treated with 0.3% Pronase (Boehringer Mannheim, Indianapolis, Ind.) and 0.1 M 2-mercaptoethanol at 4 °C to detach cells and strip surface-bound proteins. Radioactivities of the entire cell suspension, and of the supernatant and precipitate after pronase stripping, were measured. The number of cells per dish was determined by harvesting cells from dishes processed in an identical manner and counting with a hemacytometer to obtain data on a per-cell basis. Data were fit by nonlinear regression to:

$$[Ab_s] = [Ab_{ss}] + [Ab_{ns}] = \frac{K[Ab][Ag_{s,total}]}{1 + K[Ab]} + K_{ns}[Ab] \quad (2)$$

where $[Ab_s]$ is the total number of antibodies bound per cell, $[Ab_{ss}]$ and $[Ab_{ns}]$ are the numbers of antibodies per cell bound specifically and nonspecifically respectively, $[Ag_{s,total}]$ is the total number of specific antibody binding sites per cell, [Ab] is the unbound antibody concentration in solution (M), K is the equilibrium constant for specific binding of antibody to antigen (M^{-1}) and K_{ns} is a pseudo-equilibrium constant for nonspecific binding (molecules/cell M).

Internalization kinetics

SK-MEL-2 cells were harvested and plated into 60-mm culture dishes as described above. After 24 h incubation at 37 °C, 5% CO_2, the supernatant was replaced with 3 ml warm medium containing 2 nM ^{125}I-labeled 9.2.27. The dishes were incubated at 37 °C for various times (10 min–24 h). The concentration of mAb in the supernatant was determined in a gamma counter (model 5002, Packard, Meriden, Conn.). Total cell-associated, surface, and internal mAb were determined essentially as described above. Material balances (total = surface + internal) were checked on all samples and agreed within a few percent. The number of cells in control dishes was measured in parallel to each kinetics experiment to establish the initial number of cells and the growth kinetics. Calculated values of total, bound, and internalized antibody were normalized to a per cell basis, using the initial cell number and Eq. 1.

Degradation assay

In 60-mm culture dishes, 5×10^5 cells in 3 ml medium were plated and then incubated for 24 h. Control dishes containing only medium without cells were incubated simultaneously. After 24 h incubation, the supernatant or medium was replaced with 3 ml fresh

warm medium containing 2 nM ^{125}I-labeled 9.2.27 and the dishes were incubated at 37 °C. At various times (1–46 h) triplicate 50-µl aliquots were removed from separate dishes. To each aliquot 450 µl 10 mg/ml bovine serum albumin and 500 µl 10% trichloroacetic acid were added. The precipitate was pelleted, and the radioactivity in the supernatant was measured by gamma counting. The nonprecipitable activity was assumed to be a measure of the extent of mAb degradation. Degradation of antibody attributed to cellular metabolism was determined by subtracting degradation in culture medium in control samples.

Construction and purification of immunotoxins

A 1-ml sample of 9.2.27 (approximately 1 mg/ml) in phosphate-buffered saline (PBS) was reacted with 10 µl *N*-succinimidyl 3-(2-pyridyldithio)propionate (SPDP; 0.7 mg/ml in DMSO) at 30 °C for 1 h. Excess SPDP was removed by dialysis against PBS. The modification resulted in the introduction of an average of 1.3 2-pyridyl disulfide groups/mAb, determined using methods in the literature [5]. A 2-mg sample of gelonin (Pierce) was dissolved in 1 ml 0.1 M Na_2PO_4/NaH_2PO_4, 1 mM EDTA, pH 8, buffer and reacted with 0.4 mg 2-iminothiolane (Pierce) at 30 °C for 30 min. The reaction mixture was applied to a 5-ml Excellulose GF-5 size-exclusion column (Pierce) pre-equilibrated with PBS + 0.6 M NaCl + 1 mM EDTA to remove excess 2-iminothiolane. Ellman's test [8] indicated that 1.7 sulfhydryl groups/gelonin were added. Modified gelonin was mixed with SPDP-modified 9.2.27 in a 4:1 molar ratio and concentrated by ultrafiltration through a YM10 membrane (Amicon). The concentrated mixture was reacted for 2 days on a rotator at room temperature, after which 0.5 mg iodoacetamide was added for 1 h to block unreacted sulfhydryl groups. Samples were dialyzed against PBS. To separate immunotoxin from unreacted antibody, samples were applied to a blue Sepharose CL-6B (Pharmacia) column equilibrated with PBS [20]. Unreacted antibody passed through the column. Gelonin-containing immunotoxin was eluted with PBS + 1 M NaCl (pH 7). Eluant was further purified by size-exclusion (GF-450) HPLC to obtain a 1:1 conjugate and verified by SDS-PAGE.

Protein synthesis inhibition

Following the manufacturer's instructions, the Promega (Madison, Wis.) rabbit reticulocyte lysate system was used to test immunotoxin activity in a cell-free system. The activity of the immunotoxin was similar to that of unconjugated gelonin. To measure protein synthesis inhibition in immunotoxin-treated cells, the procedure previously described [34] was used with minor alterations. Briefly, 100 µl cell suspension (4×10^3 cells) was added to each well of a 96-well plate and incubated for 24 h to allow cells to attach. Medium was removed and replaced with 100 µl medium containing various concentrations of immunotoxin and 10% PBS. After incubation of the cells with immunotoxin for 24–91 h, the supernatant was replaced with 50 µl leucine-free medium containing 1.7 µCi [^{3}H]leucine. After 1 h incubation, monolayers were washed with 5% trichloroacetic acid, then cells were dissolved with 0.1 M KOH, and [^{3}H]leucine incorporated into protein was measured by scintillation counting.

Results

Binding affinity

Cell-associated 9.2.27 as a function of antibody concentration was measured at 4 °C after incubation for 0.5–1 h (Fig. 1A). At 100-fold molar excess of unlabeled 9.2.27 there was no measurable cell-associated radioactivity (not shown), so the data were fit to Eq. 2 with K_{ns} set equal to 0. Values of $K = 1 \pm 0.1 \times 10^{10}$ M^{-1} and $[Ag_{s,total}] = 3.9 \pm 0.2 \times 10^5$ binding sites/cell were obtained. The measured binding affinity at 4 °C is consistent with a previously reported value of $3 \pm 2 \times 10^{10}$ M^{-1} [28]. Binding experiments with Fab fragments of 9.2.27 produced similar estimates of K and $[Ag_{s,total}]$ (data not shown), indicating that 9.2.27 binds univalently to HMW-MAA. At 37 °C, binding data were collected after 0.5–1 h incubation (Fig. 1B) at which time the influence of metabolic activity on the amount bound should be negligible (see next section). Under the conditions of this assay, there was some cell-associated radioactivity in the presence of excess unlabelled 9.2.27 at concentrations above about 10 nM 9.2.27 (data not shown), therefore, the fit of the binding data at 37 °C to Eq. 2 included nonspecific binding. Values of $K = 9 \pm 2 \times 10^8$ M^{-1}, $K_{ns} = 3 \pm 0.2 \times 10^{12}$ (binding sites/cell, M) and $[Ag_{s,total}] = 2.4 \pm 0.1 \times 10^5$ sites/cell were obtained. The decrease in K with temperature is consistent with a constant ΔG (Gibbs free energy) of binding, if $\ln K = -\Delta G/RT$, with $\Delta G = -53.3$ kJ/mol. $[Ag_{s,total}]$, the number of antibody binding sites at saturation, exhibited some assay-to-assay variability but was generally $4 \pm 2 \times 10^5$ sites/cell. Variation in HMW-MAA expression levels has been

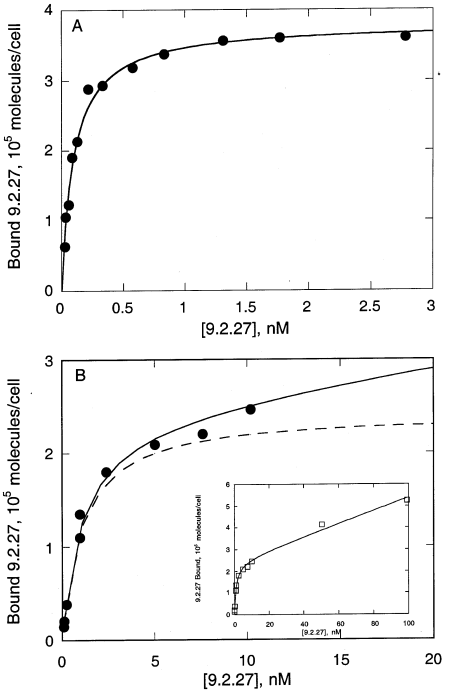

Fig. 1A, B 9.2.27 binding to SK-MEL-2. SK-MEL-2 monolayers were incubated with various concentrations of ^{125}I-labeled 9.2.27 and surface and medium concentrations were determined. **A** 4 °C. Data points are individual measurements from a single experiment. Fit of data to Eq. 2, with $K_{ns} = 0$. K determined from other similar experiments was similar to that shown here, but $[Ag_{s,total}]$ varied from run to run. **B** 37 °C. Data are individual measurements from two separate experiments. — Fit of data to Eq. 2, - - - the calculated specifically bound antibody, $[Ab_{ss}]$. *Insert* data for a wider range of 9.2.27 concentration

observed by others [28] and is strongly dependent on factors such as culture density and feeding schedule [18].

Internalization and degradation kinetics

SK-MEL-2 monolayers were incubated at 37 °C with 9.2.27 at the subsaturating concentration of 2 nM or at the saturating concentration of 20 nM. Total cell-associated, pronase-sensitive (presumably surface-bound), and pronase-resistant (presumably internalized) antibody were measured as a function of time; the data are plotted on a per dish and per cell basis (Figs. 2 and 3). Surface radioactivity (bound radioactivity per dish) was essentially constant over this period (Fig. 2B) at both concentrations. However, because cell growth occurred, the amount of surface-bound antibody per cell decreased (Fig. 2A). Binding of the antibody to the cell surface was rapid, reaching a maximum in 15–30 min. At 2 nM, the number of bound antibodies decayed from approximately (2.5–3) $\times 10^5$ initially to around (1.4–1.7) $\times 10^5$ antibodies/cell over 24 h, the small difference between the two experiments being attributable to variable antigen expression levels, as described above. At 20 nM, surface antibody decreased from about 6.5×10^5 to about 5.5×10^5 antibodies/cell over the same period. The internal (pronase-resistant) radioactivity per dish increased over a period of about 5 h, then leveled-off (Fig. 3A). A control experiment conducted at 4 °C indicated that there was no cell-associated radioactivity following pronase stripping, which is to be expected if the internalization results from cellular metabolic activity. At 2 nM, the intracellular antibody on a per cell basis increased and then leveled-off; at 20 nM, the amount of intracellular antibody per cell reached a maximum at about 5 h and then decreased slightly. To look at longer-term effects, SK-MEL-2 cells were incubated with 2 nM or 10 nM 9.2.27 for 24 h or 48 h; there was no significant change in the amount of surface or internal antibody per cell over this period, indicating that the system had reached approximately steady-state at 24 h (data not shown). Monolayers were incubated with 9.2.27 at concentrations from 0.1 nM to 20 nM for 24 h. As shown in Fig. 4, there was a linear relationship between internal and surface-bound antibody over this concentration range.

Degradation of 2 nM 9.2.27 by SK-MEL-2 cells was measured over a 46-h period by assessing the fraction of radioactivity that was not precipitable by trichloroacetic acid in the presence of cells compared to that in medium

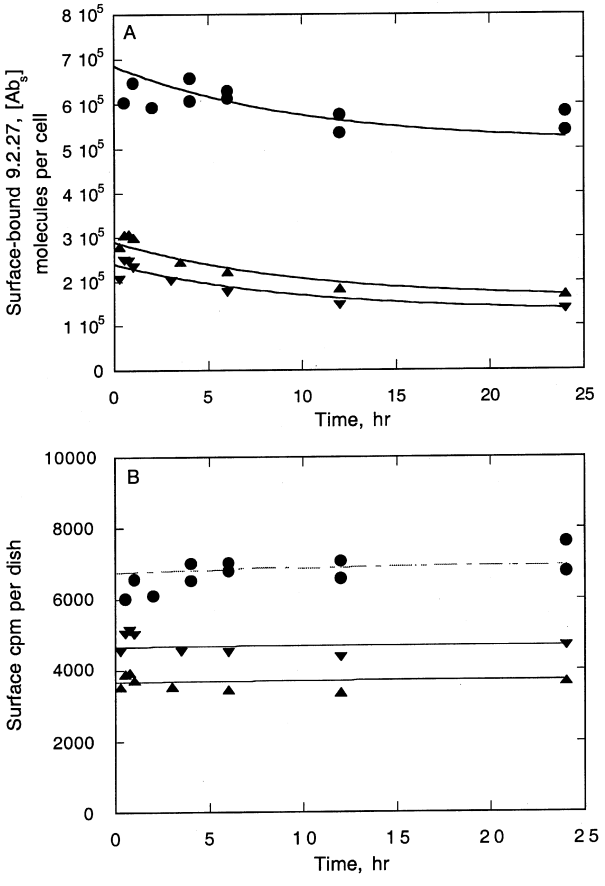

Fig. 2A, B Kinetics of 9.2.27 binding. SK-MEL-2 monolayers were incubated with 2 nM (▲, ▼, representing two independent experiments) or 20 nM (●) at 37 °C for various periods of time, and surface-bound (Pronase-sensitive) 9.2.27 was determined. **A** Surface-bound 9.2.27 per cell, calculated from surface radioactivity per dish; calibration curve for 9.2.27 (cpm/μg), cell growth curve (Eq. 1), and experimentally determined initial cell number. **B** Surface radioactivity per dish. Lines are calculated from Eqs. 1–5 with $k_i = 2.5 \times 10^{-4}$ min^{-1} and $k_d = 6 \times 10^{-3}$ min^{-1}

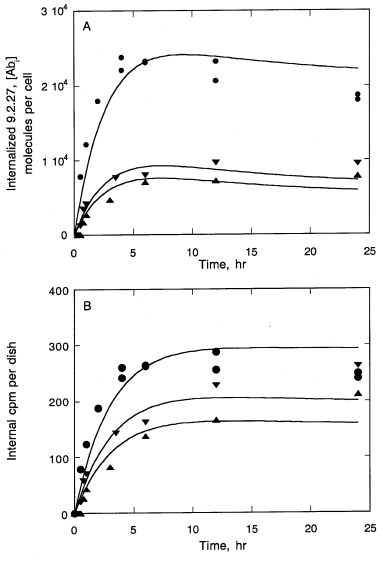

Fig. 3A, B Kinetics of 9.2.27 internalization. SK-MEL-2 monolayers were incubated with 2 nM (▲, ▼, representing two independent experiments) or 20 nM (●) 9.2.27 at 37 °C for various periods of time. Intracellular (Pronase-resistant) 9.2.27 was determined as described in Materials and methods. **A** Intracellular 9.2.27 per cell, calculated from internal radioactivity per dish; calibration curve for 9.2.27 (cpm/μg), cell growth curve (Eq. 1), and experimentally determined initial cell number. **B** Internal radioactivity per dish. Lines are calculated from Eqs. 1–5 with $k_i = 2.5 \times 10^{-4}$ min^{-1} and $k_d = 6 \times 10^{-3}$ min^{-1}

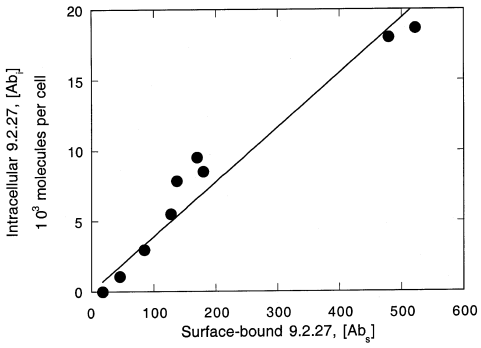

Fig. 4 Surface and internal 9.2.27 at 24 h. SK-MEL-2 monolayers were incubated with 0.1–20 nM ^{125}I-labeled 9.2.27 for 24 h, at which point surface-bound and intracellular concentrations were determined. Data were converted to a per cell basis using the measured cell count at 24 h. *Line* linear fit to the data through the origin

without cells. After 24 h, about 1% of the antibody was degraded and, after 46 h, about 2.5% was degraded by cellular activity.

Cellular trafficking model

We relied on these observations to derive a simple model of mAb 9.2.27 processing by SK-MEL-2 cells. Binding of 9.2.27 to surface antigens was rapid; therefore, we postulated that association and dissociation rates are much faster than those of other cellular processes and that, to a reasonable approximation, free antibody in the medium is always in equilibrium with antibody bound to cell-surface antigens. We assumed further that surface-bound antibody is internalized, and, once internalized, routed to a degradation pathway. Because HMW-MAA is not actively endocytosed as a normal mechanism for uptake of ligands, we assumed that none of the internalized antibody is rerouted to the cell surface. This can be expressed in differential form as

$$\frac{\mathrm{d}[\mathrm{Ab_i}]}{\mathrm{d}t} = k_\mathrm{i}[\mathrm{Ab_s}] - k_\mathrm{d}[\mathrm{Ab_i}] \tag{3}$$

where $[\mathrm{Ab_i}]$ is the number of internal antibodies per cell, and k_i and k_d are first-order rate constants for internalization and degradation respectively. Note that k_i could be a lumped parameter that incorporates the intrinsic internalization rate and the fraction of surface-bound antigen that is internalization-competent. We assume that this is constant.

Loss of antibody in the medium as a result of lysosomal degradation is expressed as

$$\frac{\mathrm{d}[\mathrm{Ab}]}{\mathrm{d}t} = -\frac{c}{N_\mathrm{A}V}k_\mathrm{d}[\mathrm{Ab_i}] \tag{4}$$

where V is the volume of medium in the dish and N_A is Avogadro's number. HMW-MAA is shed into the medium, although the level varies with the cell line and culture conditions [7, 9, 23]. To determine whether there was any decrease in free antibody concentration as a result of binding of the antibody to antigen shed from cells into the medium, spent medium was collected after 48 h incubation with SK-MEL-2 cells. A subsaturating concentration of ^{125}I-labeled 9.2.27 was added to either fresh medium or spent medium, then incubated with fresh cells, and the amount of cell-associated antibody was measured. There was no difference in antibody binding fresh and spent medium (data not shown). This indicates that, if any antigen is shed from the cells, it is either unable, or in insufficient quantities, to bind measurable amounts of antibody in the medium, and therefore no term accounting for this effect is required.

We observed that cell-surface-bound antibody decreased with time (Fig. 2A). This was not due to a decrease in [Ab], as the antibody concentration in the medium remained constant, within experimental error, over the course of the experiment (data not shown). Nor could this be attributed to effects of antibody on cell growth, since cell growth kinetics were identical in the absence or presence of 2 nM or 10 nM 9.2.27 (data not shown). Antigen expression did not decay to zero, since at 48 h the amount of surface-bound 9.2.27 was similar to that at 24 h. Thus, there appears to be a decrease in antigen density per cell to a new steady-state level. Given the observation that the total surface radioactivity *per dish* remained essentially constant, even though the surface-bound 9.2.27 *per cell* decreased (Fig. 2), we modelled the antigen density as:

$$[\mathrm{Ag_{s,total}}]c = [\mathrm{Ag_{s,total}}]_0 c_0 \tag{5}$$

where $[\mathrm{Ag_{s,total}}]_0$ is the initial antigen density per cell. $[\mathrm{Ag_{s,total}}]$ is then calculated at any time t by combining Eq. 1 and Eq. 5. The mechanism by which the total antigen number per dish remains constant is not specified in this formulation but is likely a net result of antigen degradation, shedding, and synthesis rates, the rates of which may depend on the number of bound antibodies, cell density, and/or other factors.

Model parameters were determined by evaluation of the experimental data. To obtain an initial estimate of k_i, the In/Sur method was used [17]. Briefly, at sufficiently early times degradation and other processes are negligible, and approximately

$$[\mathrm{Ab_i}] = k_\mathrm{i}\int_0^t [\mathrm{Ab_s}]\mathrm{d}t \tag{6}$$

The integral of $[\mathrm{Ab_s}]$ over time was evaluated numerically at several times and plotted against $[\mathrm{Ab_i}]$ at that time. For the data at 2 nM, a straight line with a slope of $k_\mathrm{i} \approx 3 \times 10^{-4}\,\mathrm{min}^{-1}$ was obtained. There were insufficient data at 20 nM at early times to obtain an estimate of k_i by this method. To estimate k_d, two approaches were taken. First, at steady state Eq. 3 reduces to

$$[\mathrm{Ab_i}] \approx \frac{k_\mathrm{i}}{k_\mathrm{d}}[\mathrm{Ab_s}] \tag{7}$$

As shown in Fig. 4, a plot of $[Ab_i]$ against $[Ab_s]$ is linear with a slope of $k_i/k_d \approx 0.04$. Using this ratio and the estimate of k_i from early times, $k_d \approx 8 \times 10^{-3}$ min^{-1}. Alternatively, on the basis of the experimentally measured increase in material not precipitable by trichloroacetic acid from 12 h to 46 h, and using Eq. 4, an estimate of $k_d \approx 3 \times 10^{-3}$ min^{-1} was obtained.

To obtain better estimates of the rate constants, k_i and k_d were simultaneously fit to the kinetic data in Figs. 2A and 3A, by the multiresponse parameter estimation package GREG [30, 31], with Eqs. 1–5 solved using the differential/algebraic equation solver DDASAC [4]. For each data set, the experimentally determined free antibody concentration [Ab] and initial cell number per dish c_0 were used as inputs. Initial antigen density $[Ag_{s,total}]_0$ was estimated for each individual data set by using Eq. 2 and extrapolating back $[Ab_s]$ measurements to $t = 0$. The best fit for all data sets combined was obtained with $k_i = 2.5 \times 10^{-4}$ min^{-1} and $k_d = 6 \times 10^{-3}$ min^{-1}, in good agreement with parameter values estimated by other means (above). Results from these calculations are plotted in Figs. 2 and 3 and show that the model captures both the per cell and per dish data reasonably well at both subsaturating and saturating concentrations. The calculated percentage of antibody degraded by cellular processes (2 nM initial antibody) was 0.7%–0.8% at 12 h and 3%–3.8% at 46 h, in good agreement with measured values obtained in independent degradation experiments.

Correlation between cellular trafficking and protein synthesis

The kinetics of protein synthesis inhibition by 9.2.27-gelonin immunotoxins were measured in SK-MEL-2 cells at initial immunotoxin concentrations of 0.1 nM, 1 nM, and 10 nM and at incubation times of 24 h, 36 h, and 48 h (Fig. 5). Minimal toxicity was observed at 0.1 nM. At 1 nM, 9.2.27-gelonin was slightly toxic, inhibiting protein synthesis to 70% of untreated cells at 48 h. At 10 nM, 9.2.27-gelonin inhibited protein synthesis to 40% of controls at 48 h.

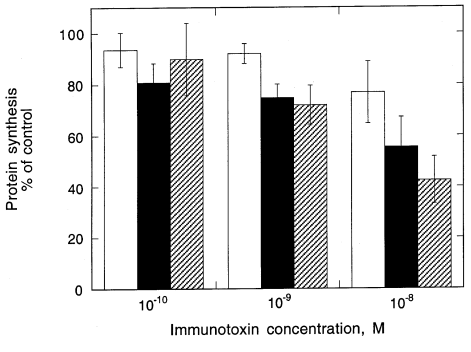

Fig. 5 Protein synthesis inhibition kinetics. SK-MEL-2 cells were incubated in medium containing 0.1, 1, or 10 nM 9.2.27-gelonin for 24 h (*open*), 36 h (*solid*) or 48 h (*striped*) and protein synthesis of immunotoxin-treated wells relative to untreated controls was determined by measuring [^{3}H]leucine incorporation. *Error bars* SD of four replicates

Previously [34, 35], it was shown that protein synthesis inhibition kinetics of gelonin immunotoxins targeted against the transferrin receptor could be simply related to the cellular trafficking kinetics of the corresponding targeting agent (transferrin or anti-TfR antibodies OKT9 and 5E9) by a single equation:

$$PS = \exp[-K_{PSI}(CTV)] \tag{8}$$

where

$$CTV = \int_0^{t_i} \int_0^{t'} [Ab_i] dt' dt \tag{9}$$

and

$$K_{PSI} = \left(\frac{k_{cat}}{K_M}\right)_{tox} k_{tr} \tag{10}$$

PS is the fraction of protein synthesis relative to control cells, measured after an exposure time t_i to the immunotoxin. CTV is the "cellular trafficking variable", defined by Eq. 9. In essence CTV represents the accumulated cytosolic exposure of the cell to the immunotoxin. K_{PSI} incorporates three constants related to the toxin: k_{cat} and K_m, Michaelis-Menten constants for the enzymatic rate of substrate inactivation by the toxin, and k_{tr}, the first-order rate constant for translocation of toxin from an intracellular compartment to the cytosol. Several assumptions underlie the derivation of Eq. 8, the chief ones being that the immunotoxin is trafficked in an identical manner to the antibody, the translocation rate is much slower than other rate constants, and the kinetics of ribosome inactivation are first-order [34].

$[Ab_i]$ as a function of time and immunotoxin concentration was numerically calculated from the trafficking model (Eqs. 1–5) using DDASAC, with c_0 and [Ab] set by the experimental conditions of the protein synthesis inhibition assay. CTV was calculated by numerical integration of Eq. 9, with t set at the experimental incubation times. The experimental data for protein synthesis (Fig. 5) in the presence of 9.2.27-gelonin was plotted against CTV (Fig. 6). The data collapse to a single curve. Equation 8 was fitted to the data by nonlinear least-squares regression, treating K_{PSI} as a parameter. K_{PSI} was determined to be $2.3 \pm 0.2 \times 10^{-11}$ molecule min^2 cell^{-1}. Using a value for k_{cat}/K_m of 7×10^8 M^{-1} min^{-1} [32], k_{tr} was estimated to be approximately 5×10^{-8} min^{-1}, or about four orders of magnitude slower than the internalization rate constant k_i.

To determine whether greater inhibition of protein synthesis could be achieved by longer incubation times, cells were incubated with 9.2.27-gelonin immunotoxins for up to 91 h, the medium being replaced with fresh immunotoxin after 48 h. Surprisingly, there was no additional decrease in protein synthesis with time, and at

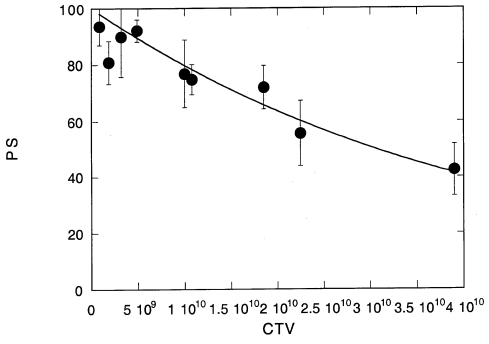

Fig. 6 Protein synthesis (PS) as a function of the cellular trafficking variable (*CTV*). CTV was calculated from Eq. 9 as described in the text. Protein synthesis was taken from the data in Fig. 5. *Line* least squares fit of the data to Eq. 8

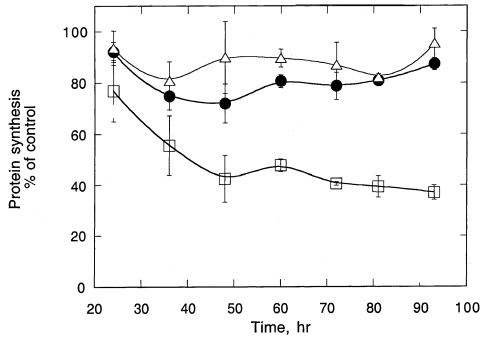

Fig. 7 Protein synthesis inhibition kinetics at long times. SK-MEL-2 cells were incubated in medium containing 0.1 nM (△), 1 nM (●) or 10 nM (□) 9.2.27-gelonin for 24–91 h and protein synthesis of immunotoxin-treated wells relative to untreated controls was determined by measuring [^{3}H]leucine incorporation. *Error bars* SD of four replicates. *Lines* simply smooth curves drawn through the data points

1 nM there may have even been a recovery back to control levels (Fig. 7). This was not due to loss of immunotoxin activity, as the immunotoxin remained active against freshly prepared monolayers (data not shown).

Discussion

Previously, this laboratory showed that protein synthesis inhibition kinetics of anti-TfR–gelonin immunotoxins were related to the cellular trafficking kinetics of transferrin or anti-TfR antibodies in HeLa and SK-MEL-2 cells [32, 33], and that Eq. 8 quantitatively characterized this relationship. In this work, we applied the same methodology to the immunotoxin, 9.2.27-gelonin, which targets the HMW-MAA, in an attempt to determine the general applicability of the model. HMW-MAA has attracted attention as a potentially useful target for immunotoxins [3, 10–13, 27, 29], as it is expressed widely on melanoma cells but not on normal or other neoplastic cells [2, 26]. Our analysis is useful for quantitative assessment of the antigen's utility as a target.

Several immunotoxins targeted at HMW-MAA have been constructed and tested, using 9.2.27 conjugated to gelonin, abrin or abrin A, ricin or ricin A, *Pseudomonas* exotoxin A, diptheria toxin A, and pokeweed antiviral protein [3, 10–13, 24, 29]. Sensitivity to the immunotoxin varied widely, depending on variables such as the cell line, incubation time, and method of preparation. The 50% inhibition doses at 20–48 h exposure times ranged from about 0.1 mM to about 10^{-5} nM. We chose gelonin as the toxic moiety because of its lack of toxicity in the absence of conjugation to a targeting antibody, and to provide a means for comparison to our previous results with TfR-directed gelonin immunotoxins. 9.2.27-gelonin conjugates were not particularly potent, requiring long incubation times (24–48 h) and doses in the 1–10 nM range before measurable inhibition of protein synthesis was observed.

A simple cellular trafficking model describing the processing of 9.2.27 by SK-MEL-2 cells was developed. To our knowledge, this is the first quantitative model of 9.2.27 processing. The model is consistent with several sets of independent data. Of particular interest is the observed decrease in antigen density, which correlated inversely with the increase in cell number. The antibody number per cell (surface plus internal) decreased with time, so a simple re-distribution of antigen from the surface to the cell interior cannot account for the observed change. We considered whether the decrease in surface antigen could be attributed to lysosomal degradation of the antigen. The affinity of 9.2.27 for surface antigen was the same if the medium was acidic (pH 5.5) or neutral (data not shown), thus, internalized antigen likely trafficks with the antibody and is degraded. From our model, we estimated that, if antigen degradation occurs at the same rate as antibody degradation with no compensatory increase in antigen synthesis, the antigen number per cell would decrease by about $(3–4) \times 10^4$, 5×10^4, and 1×10^5, after 12 h, 24 h, and 48 h respectively, at 2 nM initial mAb concentration. Experimentally, the greatest decrease in antigen density was observed at earlier times, when intracellular antibody levels, and hence degradation rates, were lowest, and little if any decrease occurred between 24 h and 48 h, when intracellular antibody levels were higher. Thus, antigenic degradation alone cannot explain the data. If HMW-MAA shedding rates increased in response to antibody binding without a concomitant increase in antigen synthesis rates, antigen density would decrease. Assuming that all the antigen is sheddable, then cell-surface binding would decay exponentially to zero, but this was not observed. Similarly, Giacomini et al. [9] observed no decrease in HMW-MAA expression per cell for Colo 38 cells in the presence or absence of antibodies, despite measurable shedding rates. The most likely explanation, we believe, is that antigen expression changes in response to increases in cell density. Lindmo et al. [18] observed that HMW-MAA density decreased to 70% of the original value in FME cells because of contact inhibition as the cells grew. HMW-MAA

expression level is likely a net result of a number of processes including antigen degradation, shedding, and synthesis. Changes in HMW-MAA expression levels correlate most simply with changes in cell number.

The internalization rate constant for 9.2.27 is much slower than that for transferrin or anti-TfR antibodies. For example, k_i for 9.2.27 in SK-MEL-2 cells is about 500-fold smaller than k_i for transferrin in the same cell line [34]. However, the degradation rate constant k_d for 9.2.27 is similar to that for anti-TfR antibodies [35]. The net result is a far lower intracellular accumulation of 9.2.27 than that of anti-TfR antibodies. 9.2.27-gelonin is as effective as Tf-gelonin against SK-MEL-2 cells at equivalent concentrations [34], (this work). This is likely due to a combination of factors. TfR and HMW-MAA are expressed at roughly equal levels on this cell line (about 4×10^5 sites/cell), but the affinity of Tf for TfR is about 30-fold lower than the affinity of 9.2.27 for HMW-MAA. At subsaturating immunotoxin concentrations, this results in lower surface binding of Tf compared to 9.2.27. However, the much more favorable internalization properties of Tf compensate for the weaker surface binding. Anti-TfR antibodies 5E9 and OKT9 have binding affinities (3×10^8–5×10^8 M) similar to that of 9.2.27, but have internalization properties similar to those of Tf [35]. The net result is that gelonin immunotoxins constructed from anti-TfR antibodies are significantly more effective than 9.2.27-gelonin immunotoxins because of their better internalization properties compared to 9.2.27. For example, to achieve 60% protein synthesis required 36 h incubation with 10 nM 9.2.27-gelonin but only 24 h with 1 nM OKT9-gelonin conjugate [35].

Despite the very different cellular trafficking kinetics of 9.2.27 and TfR-targeting agents, Eq. 8 describes the 9.2.27-gelonin protein synthesis inhibition data well, indicating that the equation may be broadly applicable. The protein synthesis inhibition constant K_{PSI} of 2×10^{-11} cells molecules^{-1} min^{-2} estimated from these data is four to tenfold greater than K_{PSI} for anti-TfR gelonin immunotoxins [34, 35] but nearly 500-fold smaller than K_{PSI} for Tf immunotoxins constructed from the diphtheria toxin mutant CRM107 [33, 34]. The enzymatic rate constants for a number of bacterial and plant toxins used in immunotoxin construction are remarkably similar [34]. Thus, differences in K_{PSI} for various immunotoxins predominantly reflect differences in translocation rates. CRM107, unlike gelonin, is capable of translocating directly across the endosomal membrane [21]. The slightly larger value of K_{PSI} for the anti-(HMW-MAA)–gelonin than that of anti-TfR–gelonin immunotoxins could indicate that 9.2.27 is routed through a somewhat more translocation-competent compartment than anti-TfR targeting agents. Still, the fact that K_{PSI} is of similar order of magnitude for gelonin immunotoxins constructed from different antibodies and targeted against two different antigens, and that it differs significantly from K_{PSI} for CRM107 immunotoxins, indicates that K_{PSI} is primarily a function of the toxin, not the targeted antigen. These results further support the validity and utility of Eq. 8.

Rigorous evaluation of Eq. 8 required a quantitative model of cellular trafficking and numerical solution of the coupled differential and algebraic equations. A simpler approximate expression can be derived by postulating that the system is at quasi-steady-state. Combining Eqs. 2, 7 and 9 and neglecting nonspecific binding, one obtains:

$$\mathrm{CTV} \approx \frac{k_i}{k_d}[\mathrm{Ag}_{s,\mathrm{total}}]\left[\frac{K[\mathrm{Ab}]}{1+K[\mathrm{Ab}]}\right]t^2 \qquad (11)$$

Equations 8 and 11 together indicate that, at the low concentrations of most interest for immunotoxin therapy ($K[\mathrm{Ab}] \ll 1$), protein synthesis levels decrease exponentially with the immunotoxin concentration and with the square of the incubation time. Given our observations that K_{PSI} is, to a first approximation, dependent only on the toxin [33–35], (this work), Eq. 8 should provide order-of-magnitude predictive capability for the efficacy of a given mAb-toxin conjugate with only a few measurements of steady-state intracellular and surface-bound concentrations of the mAb.

Surprisingly, 9.2.27-gelonin immunotoxins lost their efficacy beyond 48 h (Fig. 7), even though the immunotoxin was replaced at that time. Antigenic modulation may be the key factor. In preliminary flow cytometry experiments (not shown), we observed that virtually all SK-MEL-2 cells expressed HMW-MAA, but the distribution was not completely homogeneous and there appeared to be a small fraction of cells that bound only small levels of 9.2.27. Lindmo et al. [19] reported similar heterogeneity in HMW-MAA expression on FME cells. 9.2.27-gelonin could exert selective pressure for cells with lower antigen expression levels; eventually, the cell population would become resistant to the immunotoxin. However, Morgan et al. [24] observed that cells treated with 9.2.27-pokeweed antiviral protein conjugates developed some resistance to all A-chain conjugates, even though the cells continued to express HMW-MAA. Thus, the reason for development of resistance remains unclear.

Acknowledgements Financial support was provided by NIH Biotechnology Training Grant 5T326M08349 and NSF BES-9417006. Grace Tan and Michael Keller provided technical assistance.

References

1. Bailey JE, Ollis DF (1986) Biochemical engineering fundamentals, 2nd edn. McGraw-Hill, New York
2. Berd D, Herlyn M, Koprowski H, Mastrangelo MJ (1989) Flow cytometric determination of the frequency and heterogeneity of expression of human melanoma-associated antigens. Cancer Res 49:6840
3. Bumol TF, Wang QC, Reisfeld RA, Kaplan NO (1983) Monoclonal antibody and an antibody-toxin conjugate to a cell-surface proteoglycan of melanoma cells suppress in vivo tumor growth. Proc Natl Acad Sci USA 80:529

4. Caracotsios M, Stewart WE (1985) Sensitivity analysis of initial value problems with mixed ODEs and algebraic equations. Comp Chem Eng 9:359–365
5. Carlsson J, Drevin H, Axen R (1978) Protein thiolation and reversible protein-protein conjugation: *N*-succinimidyl 3-(2-pyridyldithio)propionate, a new heterobifunctional reagent. Biochem J 173:723
6. Ciechanover A, Schwartz AL, Dautry-Varsat A, Lodish HF (1983) Kinetics of internalization and recycling of transferrin and the transferrin receptor in a human hepatoma cell line. J Biol Chem 258:9681
7. Davies CDL, Lindmo T (1990) Hyperthermia-induced shedding and masking of melanoma-associated antigen. Int J Hyperthermia 6:1053
8. Ellman GL (1959) Tissue sulfhydryl groups. Arch Biochem Biophys 82:70
9. Giacomini P, Natali P, Feroone S (1985) Analysis of the interaction between a human high molecular weight melanoma-associated antigen and the monoclonal antibodies to three distinct antigenic determinants. J Immunol 135:696
10. Godal A, Fodstad O, Morgan AC, Pihl A (1986) Human melanoma cell lines showing striking inherent differences in sensitivity to immunotoxins containing holotoxins. J Natl Cancer Inst 77:1247
11. Godal A, Fodstad O, Phil A (1987) Studies on the mechanism of action of abrin-9.2.27 immunotoxin in human melanoma cell lines. Cancer Res 47:6243
12. Godal A, Fodstad O, Pihl A (1988) Kinetics of uptake and degradation of an abrin immunotoxin by melanoma cells and studies of the rates of cellular intoxication. Int J Cancer 42:400
13. Godal A, Kumle B, Pihl A, Juell S, Fodstad O (1992) Immunotoxins directed against the high-molecular-weight melanoma-associated antigen. Identification of potent antibody-toxin combinations. Int J Cancer 52:631
14. Harper JR, Reisfeld RA (1983) Inhibition of anchorage-independent growth of human melanoma cells by a monoclonal antibody to a chondroitin sulfate proteoglycan. J Natl Cancer Inst 71:259–263
15. Harper JR, Quaranta V, Reisfeld RA (1986) Ammonium chloride interferes with a distinct step in the biosynthesis and cell surface expression of human melanoma-type chondroitin sulfate proteoglycan. J Biol Chem 261:3600
16. Iida J, Meijne AML, Spiro RC, Roos E, Furcht LT, McCarthy JB (1995) Spreading and focal contact formation of human melanoma cells in response to the stimulation of both melanoma-associated proteoglycan (NG2) and $\alpha 4\beta 1$ integrin. Cancer Res 55:2177
17. Lauffenburger DA, Linderman JJ (1993) Receptors: models for binding, trafficking and signaling. Oxford University Press, New York p 89
18. Lindmo T, Davies C, Rofstad EK, Fodstad O, Sundan A (1984) Antigen expression in human melanoma cells in relation to growth conditions and cell-cycle distribution. Int J Cancer 33:167
19. Lindmo T, Davies C, Fodstad O, Morgan AC (1984) Stable quantitative differences of antigen expression in human melanoma cells isolated by flow cytometric cell sorting. Int J Cancer 34:507
20. Masuda K, Hirano K, Tagakishi Y (1994) Use of blue-Sepharose for purification of immunotoxin containing type-1 ribosome-inactivating protein, gelonin. Biomed Chromatogr 8:9
21. Menestrina G, Schiavo G, Montecucuco C (1994) Molecular mechanisms of action of bacterial protein toxins. Mol Aspects Med 15:113
22. Morgan AC Jr, Galloway DR, Reisfeld RA (1981) Production and characterization of monoclonal antibody to a melanoma specific glycoprotein. Hybridoma 1:27
23. Morgan AC Jr, Galloway DR, Imai K, Reisfeld RA (1981) Human melanoma-associated antigens: role of carbohydrate in shedding and cell surface expression. J Immunol 126:365
24. Morgan AC Jr, Bordonaro J, Pearson JW, Sivam G (1987) Immunotoxins to a human melanoma-associated antigen: resistance to pokeweed antiviral protein conjugates in vitro. J Natl Cancer Inst 78:1101
25. Pluschke G, Vanek M, Evans A, Dittmar T, Schmid, Itin P, Filardo EJ, Reisfeld RA (1996) Molecular cloning of a human melanoma-associated chondroitin sulfate proteoglycan. Proc Natl Acad Sci USA 93:9710
26. Saxton RE, Mann BD, Morton DL, Burk MW (1982) Monoclonal antibodies to 125 kd and 95 kd proteins on human melanoma cells: comparison with other monoclonal defined melanoma antigens. Hybridoma 1:433
27. Schrappe M, Bumol TF, Apelgren LD, Briggs SL, Koppel GA, Markowitz DD, Mueller BM, Reisfeld RA (1992) Long-term growth suppression of human glioma xenografts by chemoimmunoconjugates of 4-desacetylvinblastine-3-carboxyhydrazide and monoclonal antibody 9.2.27. Cancer Res 52:3838
28. Shockley TR, Mandeville JT, Tompkins RG, Yarmush ML (1990) Equilibrium binding characteristics of monoclonal antibodies recognizing melanoma cell surface antigens. Hybridoma 9:527
29. Sivam G, Pearson JW, Bohn W, Oldham RK, Sadoff JC, Morgan AC Jr (1987) Immunotoxins to a human melanoma-associated antigen: comparison of gelonin with ricin and other A chain conjugates. Cancer Res 47:3169
30. Stewart WE (1987) Multiresponse parameter estimation with a new and noninformative prior. Biometrika 74:557
31. Stewart WE, Sorensen JP (1981) Bayesian estimation of common parameters from multiresponse data with missing observations. Technometrics 23:131
32. Trowbridge IS, Omary MB (1981) Human cell surface glycoprotein related to cell proliferation is the receptor for transferrin. Proc Natl Acad Sci USA 78:3039
33. Wenning LA, Yazdi PT, Murphy RM (1998) Quantitative analysis of protein synthesis inhibition and recovery in CRM107 immunotoxin-treated HeLa cells. Biotechnol Bioeng 57:484
34. Yazdi PT, Murphy RM (1994) Quantitative analysis of protein synthesis inhibition by transferrin-toxin conjugates. Cancer Res 54:6387
35. Yazdi PT, Wenning LA, Murphy RM (1995) Influence of cellular trafficking on protein synthesis inhibition of immunotoxins directed against the transferrin receptor. Cancer Res 55:3763